THE JOURNAL OF PHYSICAL CHEMISTRY B

ARTICLE

pubs.acs.org/JPCB

Nonspecific Interaction between DNA and Protein allows for Cooperativity: A Case Study with Mycobacterium DNA Binding Protein

Abantika Ganguly,[†] Priya Rajdev,[‡] Sunanda Margrett Williams,[†] and Dipankar Chatterji*[,†]

[†]Molecular Biophysics Unit, Indian Institute of Science, Bangalore 560012, India

Supporting Information

ABSTRACT: Different DNA-binding proteins have different interaction modes with DNA. Sequence-specific DNA−protein interaction has been mostly associated with regulatory processes inside a cell, and as such extensive studies have been made. Adequate data is also available on nonspecific DNA−protein interaction, as an intermediate to protein's search for its cognate partner. Multidomain nonspecific DNA−protein interaction involving physical sequestering of DNA has often been implicated to regulate gene expression indirectly. However, data available on this type of interaction is limited. One such interaction is the binding of DNA with mycobacterium DNA binding proteins. We have used the Langmuir−Blodgett technique to evaluate for the first time the kinetics and thermodynamics of *Mycobacterium smegmatis* Dps1 binding to DNA. By immobilizing one of the interacting partners, we have shown that, when a kinetic bottleneck is applied, the binding mechanism showed cooperative binding (n = 2.72) at lower temperatures, but the degree of cooperativity gradually reduces (n = 1.38) as the temperature was increased. We have also compared the kinetics and thermodynamics of sequence-specific and nonspecific DNA−protein interactions under the same set of conditions.

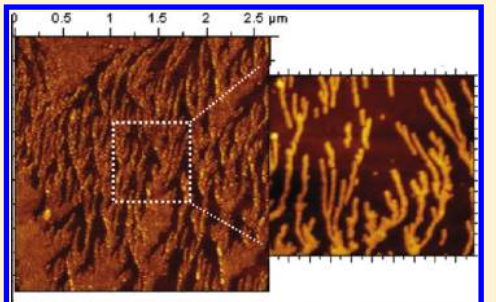

AFM Image of Two-Dimensional Network formed by His-MsDps1-DNA at the LB Monolayer

INTRODUCTION

DNA−protein interaction in a cellular organism plays a major spatial and temporal role with respect to the development of the organism. Different DNA-binding proteins have different interaction modes with DNA. In the case of sequence-specific DNA−protein interactions,[1] it involves special structural motifs on the protein[2] which is recognized by consensus sequences on the DNA[3] strand. It may involve the interaction of double-stranded DNA with a single binding site on the protein, viz., RNA polymerase−protein interaction[4] or nuclease−DNA interaction, or it may involve multiple sequence-specific binding of DNA to a repetitive motif on the protein, viz., transcription regulatory factors binding to DNA.[5] A nonspecific DNA−protein interaction, on the other hand, only involves a general affinity of the protein for a large DNA strand. It predominantly involves only ionic interactions with the sugar−phosphate backbone of DNA. Most proteins that undergo site-specific binding with DNA also share an appreciable affinity for nonspecific DNA sequences.[6] However, there are also DNA-binding proteins which have multiple binding domains that only bind to DNA nonspecifically, giving rise to large supramolecular structures. It is mostly seen in the case of genome organization or physical protection where multiple binding to a long DNA strands allows it to be condensed and made inaccessible to other environmental factors, viz., histone−DNA interaction and other structural DNA-binding proteins interacting with DNA .[7] Extensive studies have been made on the mechanism of sequence-specific DNA−protein interactions[8−10] and nonspecific interactions as an intermediate to site-specific DNA recognition.[11] However, although physical sequestering of DNA has been indirectly linked to gene regulation,[12] fundamental information on the kinetics and thermodynamics of such DNA−protein interaction is only yet emerging.

In recent years probing ligand−analyte interactions on an immobilized support is fast emerging as a powerful alternative to conventional biochemical methods.[13,14] The advantage of immobilizing one of the interacting partners, in comparison to following interactions in an ideal dilute solution, lies in the ability to emulate the crowded cellular milieu, which will provide a more practical understanding of the cellular working mechanisms *in vivo*.[15] By reducing the degrees of freedom of the reaction one is able to achieve high surface density of molecules, while overcoming the problems of precipitation associated with a high collisonal frequency. One such immobilization technique is the Langmuir−Blodgett (LB) technique.[16,17] It detects macromolecular interactions by observing changes in instantaneous surface tension responses ($\gamma_0 - \gamma$), when two partners interact at the interface.[18] As compared to other immobilization techniques, the LB method provides a unique physiologically compatible template, so as to preserve the activity of the biological molecules.[19] The ionic strength of the assays can also be regulated within cellular limits. Further, the binding parameters can be

Received: September 29, 2011
Revised: November 15, 2011
Published: November 17, 2011

evaluated under equilibrium conditions despite the nonhomogeinity of the method used.

In the recent past our laboratory has used the LB technique extensively in characterizing and evaluating protein−protein/protein−DNA interactions in an artificially crowded environment.[20,21] Previously we had developed the LB technique to evaluate the kinetic and thermodynamic parameters of sequence-specific interaction between *Escherichia. coli* RNA polymerase and T7A1 promoter DNA.[22] In the present study we have used the same technique to follow the kinetics as well as thermodynamics governing the nonsequence-specific DNA−protein interaction. The use of the same binding assay provides us with a common platform to effectively compare the differential mechanism of sequence-specific and nonspecific DNA binding. We have selected DNA binding protein from starved cells of *Mycobacterium smegmatis* (MsDps1) for our study.

DNA-binding protein from stationary phase cells (Dps) belongs to the family of nucleoid proteins which has been shown to play an important role in protecting microorganisms from oxidative or nutritional stress.[23] The protein was first identified and characterized in *Escherichia coli*.[24,25] In our laboratory, we have reported the presence of a Dps homologue in *Mycobacterium smegmatis*, MsDps1.[26] It exists in two stable oligomeric states in vitro, trimer and dodecamer. The conversion of Dps from its trimeric to dodecameric form takes place upon incubation at 37 °C for 12 h. Both the dodecamer and trimer possess the ability to carry out ferroxidation activity.[27] When a micro-organism is under stress it releases reactive oxidative species which are harmful to the cellular organism.[28] One of the reactions which releases such moiety inside the cell is Fenton's Reaction. Fe(II) undergoes Fenton's reaction to produce hydroxyl radicals ($OH^{\bullet}$) as shown in eq 1.

$$Fe^{2+} + H_2O_2 \rightarrow Fe^{3+} + OH^{\bullet} + OH^{-} \quad (1)$$

The highly negatively charged core of MsDps sequesters Fe(II) ions and converts them to Fe(III) ions.[29] But the two oligomeric forms differ in their ability to bind DNA. The dodecamer is capable of binding DNA forming highly ordered crystalline arrays, while the trimeric form is unable to bind DNA.[27] The dodecameric form can thus provide physical protection to DNA from oxidative stress and help in the survival of the organism. Using the LB technique we have, for the first time, evaluated the binding parameters and free energy of reaction for MsDps1−DNA binding, which will give us a better insight into understanding how it provides protection to DNA. Further, we have been able to show, when kinetic bottlenecks are applied, multidomain DNA−protein interactions show cooperative behavior as opposed to single-site protein−DNA binding, which follows a noncooperative model. In this context, we have also compared sequence-specific and nonspecific DNA−protein interaction to get a better insight into the underlying differences in the dynamic response of structural proteins and regulatory proteins toward their DNA recognition.

MATERIALS AND METHODS

Purification of MsDps1 and Phage DNA. His-MsDps1 was purified as described earlier.[27] Briefly, *Escherichia coli* strain BL21 (DE3) was transformed with the vector pET-ms-dps, and these cells were then grown at 37 °C in LB medium until optical density at 600 nm reached a value of 0.5. At this point, the cells were induced with 1 mM isopropyl-1-thio-β-D-galactopyranoside, and the cells were grown for an additional 3 h. The pET-ms-dps construct carries a base sequence encoding for six histidine residues at its C-terminal end. Purification was performed in a single step using the Qiagen nickel−nitriloacetic Acid (Ni-NTA) affinity matrix. The protein remained bound to the column due to the affinity of the histidine residues for Ni(II). The protein was then eluted using an elution buffer (50 mM Tris-HCl, pH 7.9 at 4 °C; 500 mM NaCl and 250 mM imidazole). The eluted fractions were pooled and precipitated using ammonium sulfate to 50% (w/v) saturation. At 50% cut, His-MsDps1 remained in the pellet after centrifugation (15,000 rpm for 15 min). The pellet was resuspended and was dialyzed overnight against 20 mM Tris−HCl (pH 7.9 at 4 °C) and 50 mM NaCl and then loaded onto an anionic diethylaminoethyl cellulose column (DE52) equilibrated with the same buffer. Pure protein was eluted using 20 mM Tris-HCl (pH 7.9 at 4 °C) and 150 mM NaCl. The purity of the protein was checked on a 15% sodium dodecylsulphate polyacrylamide (SDS-PAGE) gel electrophoresis (Figure S1 of Supporting Information). The concentration of the protein was determined using Bradford's assay at 2 mg/mL, and it was found to be fully active in catalyzing the ferroxidation reaction in vitro. The protein is always obtained as a trimer on purification at 4 °C. The trimer, when incubated at a concentration of 2 mg/mL at 37 °C for 12 h in 50 mM Tris-HCl (pH 7.9), 150 mM NaCl, was converted into its dodecameric form[27] (Figure 1), which has been used for our DNA−protein interaction studies, unless otherwise specified.

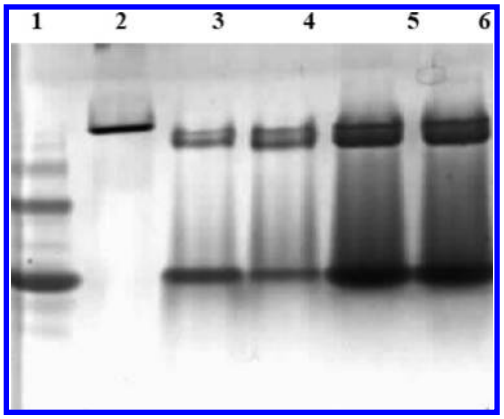

Figure 1. 10% native PAGE of His-MsDps1 to check the oligomeric status of MsDps. Lane 1, BSA; lane 2, horse spleen ferritin; lane 3, His-MsDps1 (2 mg/mL) purified at 4 °C in 50 mM Tris-HCl (pH 7.9) and 150 mM NaCl; lane 4, His-MsDps1 (2 mg/mL) in 50 mM Tris HCl (pH 7.9) and 150 mM NaCl, after incubation at 37 °C for 12 h; lane 5, His-MsDps1 (20 mg/mL) purified at 4 °C in 50 mM Tris-HCl (pH 7.9) and 150 mM NaCl; lane 6, His-MsDps1 (20 mg/mL) in 50 mM Tris-HCl (pH 7.9) and 150 mM NaCl, after incubation at 37 °C for 12 h.

For observing interactions at the Langmuir monolayer, we have used double-stranded DNA from T7 bacteriophage (39,336 base pairs). It was prepared using the protocol adapted from Nierman and Chamberlin.[30]

Native PAGE To Determine The Oligomeric State of Hexahistidine-Tagged MsDps. A 10% acrylamide native PAGE was run to study the oligomeric status of the protein. It was prepared according to the method of Laemmli.[31] The gel composition was the same except SDS was not added so that the proteins are no longer denatured but run in their native states and according

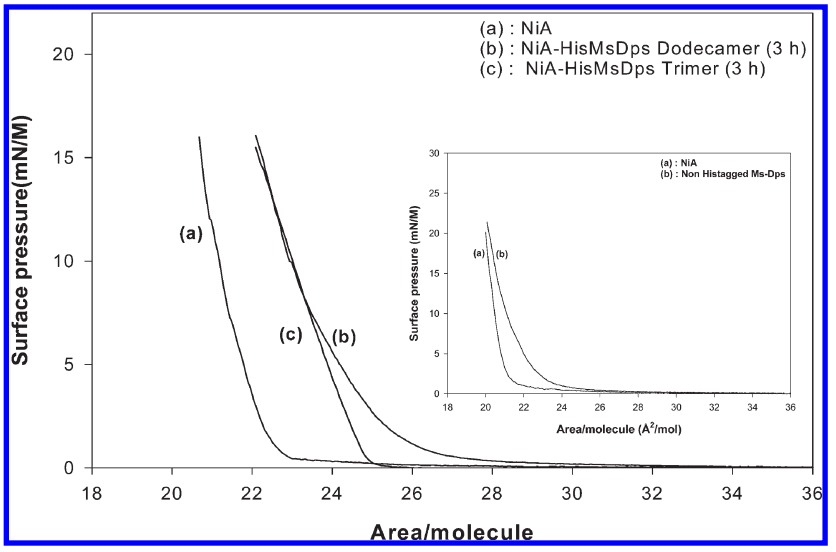

Figure 2. From left to right $P-A$ isotherms of (a) NiA, (b) 37 pmoles of His-MsDps1 dodecamer, and (c) 37 pmoles of His-MsDps1 trimer. (Inset) $P-A$ isotherms of (a) NiA and (b) non-His-tagged MsDps1 dodecamer. The His-MsDps1 was immobilized in the presence of 20 mM NaCl 30 min after the NiA monolayer is formed, and the $P-A$ isotherms were followed for additional 3 h.

to their pI values. Samples were loaded with the dye (mixture of 10% glycerol and 0.002% bromphenol blue), while the electrophoresis was carried out at a constant current of 15 mA in the presence of TG buffer (25 mM Tris at pH 8.6 and 192 mM Glycine). Bovine serum albumin (BSA, mol wt 63 kDa) and horse spleen ferritin (mol wt 450 kDa) were used as markers because they have pI close to that of the His-MsDps1 protein (pI for MsDps1 is 4.5; pI BSA is 4.6; pI horse spleen ferritin is 4.79).

Formation of LB Monolayer and Films. The monolayer was formed on a LB trough (purchased from Nima technology, U.K.). Arachidic acid, nickel sulfate ($NiSO_4$), and ferrous sulfate ($FeSO_4$) (all the chemicals were of purity 99%) were purchased from Sigma-Aldrich. The subphase was ultra pure water (Milli-Q, resistivity 18.2 MΩ cm) containing $NiSO_4$ at a concentration of 10^{-4} M. The pH of the subphase solution was maintained at 7.4 at 20 °C with 2 mM Tris-HCl (Sigma) buffer system so that the carboxyl groups remain fully ionised.[32] The monolayer was formed by spreading 25 μL of 1 mg/mL arachidic acid, dissolved in chloroform (HPLC grade, Merck), on 200 mL of subphase solution. The temperature of the trough was maintained at $t \pm 0.1$ °C with the help of a thermostat bath attached to the trough. The trough was placed under a Perspex box to avoid any dust. The readings were noted after 30 min of spreading of the surfactant solution to allow the solvent to evaporate. The barrier speed for performing all the $P-A$ isotherms was 20 cm^2/min, and all the isotherms were repeated several times to check for hysteresis. For the immobilization of His-MsDps1, we injected the protein into the aqueous subphase, below the preformed NiA monolayer. Similarly for the NiA-His-MsDp1s-DNA monolayer, the DNA was injected once the NiA-His-MsDps1 monolayer was formed. There was no stirring of the subphase after the injection of protein or DNA solution. For the kinetic studies, a set of $P-A$ isotherms were generated by injecting increasing amounts of DNA into the subphase until it reached equilibrium. The area per molecule values used for calculating the kinetic data were estimated at 25 °C and at a surface pressure of 12 mN/m, when the isotherms had reached their condensed phase. For the calculating the thermodynamic parameters, the temperature range used for the studies was 15−37 °C. Above this temperature range, experiments could not be performed due to evaporation from the subphase.

Ferroxidation Assay. First, the monolayer of NiA-HisMsDps1 was transferred onto glass slides as described before. Subsequently, a section on the glass chip was marked, and it was incubated with a small amount of freshly prepared $FeSO_4$ (10 μM) for varying time periods (1, 2, 3, and 4 min) at room temperature. At each of these time points, a small amount of the sample solution was picked up from the glass slide, and the optical density (OD) at 305 nm was measured (OD_{305}) on a NanoDrop Spectrophotometer. Fe(II) species does not absorb at 305 nm; thus, the OD_{305} obtained represents the oxidation of Fe(II) to Fe(III). To assay the bulk phase ferroxidation activity, MsDps1 in solution (5 μM) with Fe(II) (10 μM) was taken as control, and OD_{305} was measured at same time points. As a control for auto-oxidation of Fe(II) to Fe(III), ferroxidation activity of only NiA LB film as well as the buffer solution without any protein was also measured in parallel.

Atomic Microscopy Imaging. The LB films were transferred onto glass slides for atomic force microscopy (AFM) imaging. The glass slides were originally hydrophilic but to avoid the nonspecific adsorption of protein molecules from the subphase onto the glass slide, we first transferred 3 layers of NiA monolayer to make the slide hydrophobic. Next, one layer of protein monolayer was specifically transferred onto the NiA slides through specific hydrophobic interaction between the carbon chains of arachidic acid (Figure S2 of Supporting Information). The LB films were then dried for 2 h in vacuum before imaging. The AFM images were taken using an Agilent 5500 series AFM with a 10 μm × 10 μm scanner in noncontact mode in air. Silicon nitride cantilevers with a spring constant of 51 N/m was used, and the cantilever was vibrated at a frequency of 190 kHz, while the scan speed was maintained at 0.8 μm/s. The images obtained were in the topography mode (512 × 512 pixels). The images were subjected to first-order flattening before analysis. Image analysis was done using the PicoImage software (Agilent Technologies).

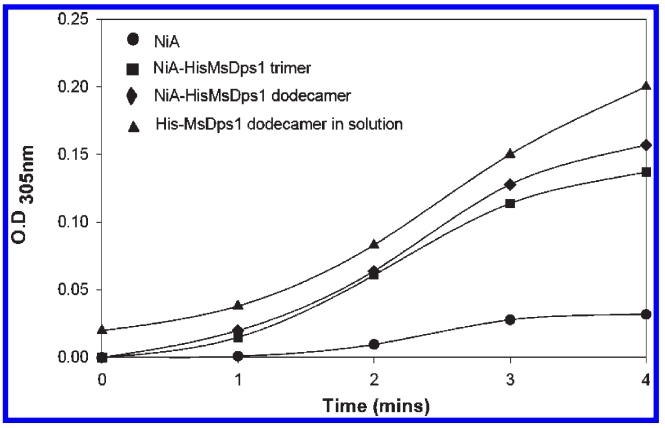

Figure 3. Ferroxidation activity measured at OD_{305}, for the LB films of (●) NiA, (■) NiA-His-MsDps1 trimer, (♦) NiA-HisMsDps1dodecamer, and (▲) His-MsDps1 dodecamer in solution.

RESULTS AND DISCUSSIONS

Immobilization of MsDps1 at NiA Monolayer. The proximate aim of this work was to array the MsDps1 protein at the interface to generate a monolayer, and to monitor the changes, if any, in the activity profile of the protein and its interaction with DNA. In our previous works, we have reported the use of Ni-arachidate-LB monolayer as a stable two-dimensional template for the purpose of immobilization of Histagged proteins and its use to follow protein−ligand interactions at the air−water interface.[20,21] The Langmuir monolayer was formed by spreading Arachidic acid solution on a subphase containing 10^{-4} M $NiSO_4$ solution at a pH of 7.4. At this pH all arachidic acid remained as arachidate ions, amenable for Ni(II) binding, to form a Ni-arachidate (NiA) monolayer at the air−water interface.[32] The free valence of the Ni(II) ions can be used for the regioselective attachment of our engineered C-terminal His-MsDps1 protein at the Langmuir monolayer. The specificity and strength of the Ni-histidine co-ordination bond used (180−200 kcal/mol) minimizes nonspecific adsorption at the interface, while allowing us to follow our desired noncovalent interactions (0.6−2.59 kcal/mol).

Protein oligomerization is sensitive to various external factors like concentration of biomolecules, ionic strength of the medium, and the presence of nonpolar additives. Hence, it is essential that the ionic strength of the medium for MsDps1 immobilization should be defined first. Previous studies conducted from our laboratory have shown that the NiA monolayer retains its monophasic properties within a salt concentration range of 0−25 mM NaCl. Increasing concentrations of monovalent Na^+ compromised the rigidity of the monolayer by lowering the condensation effect of a divalent ion like Ni^{2+}. We had characterized the same both spectroscopically and thermodynamically.[32] We immobilized His-tagged Ms-Dps1 on the NiA mnolayer, in the presence of 20 mM NaCl. Figure2 shows the *P*−*A* isotherms of NiA-MsDps1 for the two oligomeric states of the protein. It is evident from the figure that both the isotherms have similar area per molecule values when the monolayer reaches condensed phase, and this was due to the fact that equivalent moles of protein was used for both the oligomeric states. Moreover, the binding follows Ni(II)-histidine interaction, and as both the forms of MsDps1 had hexa-histidine tag attached to their C-termini, it can be reasonably assumed that the two oligomeric states will bind equivalent number of Ni(II) in the monolayer. Crystal structure has shown that His-MsDps1 possess a highly negatively charged core which sequesters Fe(II) ions. To rule out the possibility of an interaction between the negatively charged core of MsDps1 and Ni(II) at the monolayer, *P*−*A* isotherms of NiA in the presence of non-His-tagged MsDps1 were also carried out. Figure 2 shows that there was no appreciable change in the area/molecule value, and the values did not alter even after prolonged incubation with non-His-tagged protein. This confirms that the protein does not bind to the LB monolayer, in the absence of Histidine tag.

The successful immobilization of His-MsDps1 at the NiA monolayer was confirmed by FTIR spectroscopy. Two peaks, amide I band (at around 1650 cm^{-1}) and amide II band (at around 1550 cm^{-1}), are indicative of the presence of protein molecules. Amide I band is due to the C═O stretch and is fundamental to all proteins as it is situated on the protein backbone, whereas amide II band is due to N—H bending. The presence of the signature band for amide I stretching frequency at 1650 cm^{-1} (Figure S3 of Supporting Information), in the LB films of both the trimer and dodecamer confirmed the incorporation of His-MsDps1 protein into the NiA monolayer. The FTIR spectrum of only NiA was used as a control. Although NiA has asymmetric COO^- stretching vibration, the aliphatic acid peak at 1540 cm^{-1} is easily distinguishable from the amide I band of peptide backbone.

Ferroxidation Activity of the Protein Monolayer. Ferroxidation is a unique property of His-MsDps1 by the virtue of which it protects DNA from the onslaught of free radicals ($OH^•$). Both the trimeric and dodecameric forms of His-MsDps1, removes Fe (II) ions by oxidizing them to Fe(III) and sequestering them within its negatively charged core, thus inhibiting Fenton's reaction mediated DNA damage. Following the immobilization of His-MsDps1 protein at the Langmuir monolayer, we wanted to determine if the catalytic center of the protein still remains accessible to carry out its ferroxidation activity. Toward this end, the LB films of NiA-His-MsDps1 monolayer for both the trimer and the dodecamer were incubated with freshly prepared $FeSO_4$ for different time points, and their OD_{305} was measured. Figure 3 shows the ferroxidation activity of both trimeric as well as dodecameric His-MsDps1. The absorbance due to the generation of Fe(III) ions increased steadily with time and reached a plateau in about 5 min. The time taken for the optical density values to reach saturation is similar to that of the assay carried out in bulk phase. This experiment is significant in that, it showed that both the forms of His-MsDps1 (trimer and dodecamer) retain their Fe(II) binding and catalytic activity, even when they were immobilized and arrayed over a LB monolayer.

DNA Binding by His-MsDps1 Monolayer. After characterizing the His-MsDps1 monolayer, we turned our attention to another property of MsDps1 class of proteins: its ability to bind to any DNA nonspecifically and provide physical protection to DNA from the onslaught of free radicals. His-MsDps1 dodecamer is known to bind DNA of variable size (100 bp to 10,000 bp) and topography (linear or circular) in a nonsequence-specific manner.[24] A 26-amino acid long C-terminal extension that contains both positively and negatively charged amino acid side chains (3 lysines and 2 arginines plus 1 aspartic acid and 3 glutamic acids) was shown to be responsible for DNA binding and condensation.[33] Although His-MsDps1 was immobilized at the NiA monolayer using a hexahisitide tag at its C-termini, the exposed tail of the protein retains sufficient mobility to

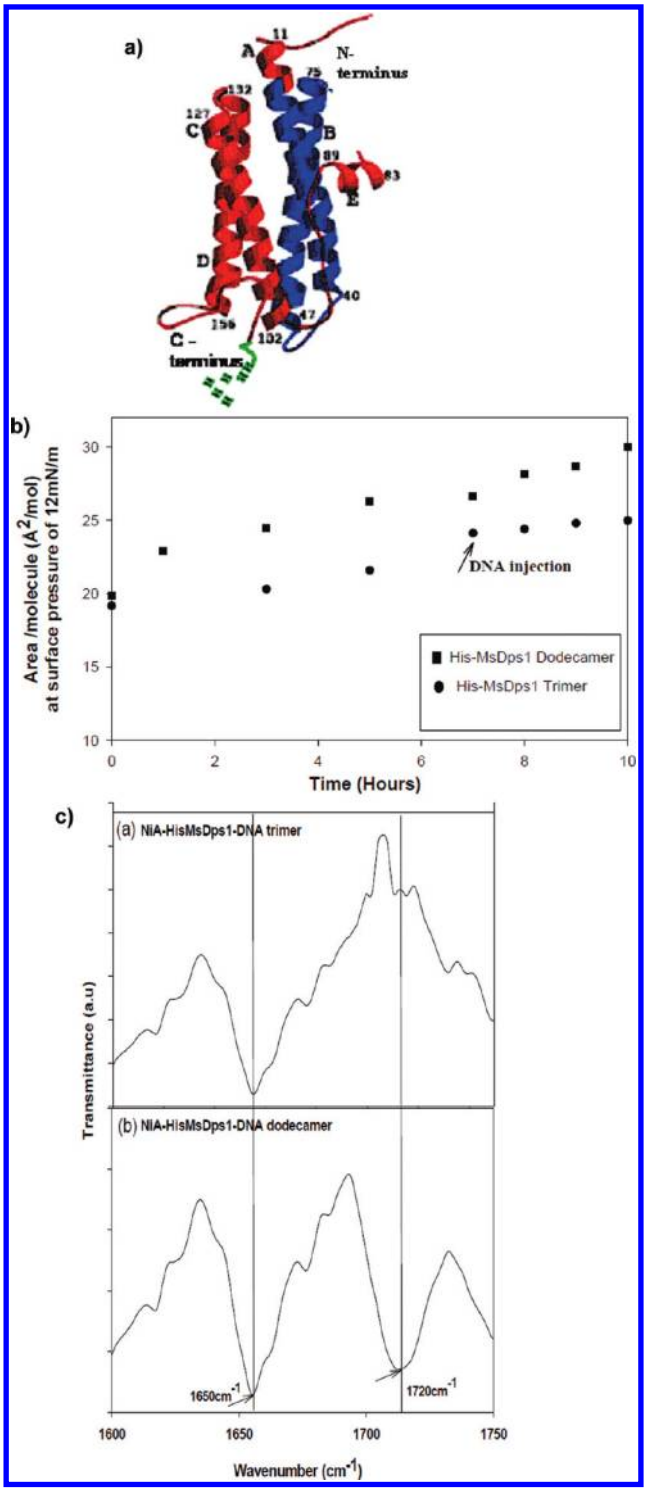

Figure 4. (a) Structure of Dps monomer unit as obtained from X-ray crystallography.[33] (b) A plot of the area/molecule vs time for (●) His-MsDps1 trimer with DNA and (■) His-MsDps1 dodecamer with DNA in a protein: DNA molar ratio of 10^3:1. The area/molecule values were determined at a fixed pressure of 12 mN/m, when the monolayer is in its condensed phase. The DNA was injected after 8 h when the protein reached equilibrium. The time of DNA injection is indicated by an arrow. (c) FTIR of LB films of (a) NiA-HisMsDps1 trimer and (b) NiA-HisMsDps1 Dodecamer. The peak at 1720 cm^{-1} corresponds to the presence of DNA.

interact with DNA (Figure 4a).[33] For our interaction study we had used here double-stranded DNA from T7 bacteriophage (39,336 base pairs), and the reason has been discussed in detail later.

To follow the DNA−protein interaction, the concentration and type of electrolyte becomes an important factor. Most *in vitro* studies of protein−nucleic acid interactions are carried out in the presence of either NaCl or KCl (within the concentrations range of 0.05−0.15 M),[34] for the purpose of mimicking the intracellular environment. However, other studies have shown that the cytoplasmic chloride content lies below this concentration spectrum.[35] The above ionic concentration range is essential for maintaining the solubility of large biomacromolecules in solution (concentration of biomolecules in the range of 0.3−1 mg/mL).[15] On the otherhand, the requirement of ionic strength at the interface is much lower to study macromolecular interactions and falls in the lower part of the optimal range.[21] To follow the His-MsDps1−DNA interaction, the salt concentration at the subphase was lowered to 10 mM NaCl. Beyond this the NiA-His-MsDps1−DNA monolayer was unstable, and we observed a biphasic collapse.

The *P*−*A* isotherms of both the trimer as well as as the dodecamer in the presence of DNA were recorded. A comparative plot of the area/molecule values, with time, at a temperature of 25 °C and a surface pressure of 12 mN/m (when the LB monolayer has reached its condense phase) was plotted for both the dodecamer and trimer in the presence of DNA. For the trimer, the *P*−*A* isotherms reached equilibrium within 7 h and did not show any further change with addition of DNA. On the other hand, for the dodecamer, we noticed that while only NiA-His-MsDps1 reached a saturation near 7 h, there was a further linear increase after the injection of DNA (Figure 4b). This clearly reconfirms the DNA binding ability of the MsDps1 dodecamer. FTIR spectra (Figure 4c) further confirmed DNA binding to dodecameric species as a peak corresponding to the presence of DNA (1720 cm^{-1}) was noticed in this case alone.

Kinetics of DNA−Protein Interaction by LB Technique. After qualitatively characterizing the DNA binding properties of His-MsDps1 dodecamer, we attempted to evaluate quantitatively the kinetic and thermodynamic parameters governing this DNA−protein interaction. In our previous work we had used T7A1 promoter containing DNA to evaluate the thermodynamics of promoter−RNA polymerase interaction.[22] The use of same DNA in this study serves the dual purpose of evaluating the MsDps1−DNA binding parameters using a nonspecific DNA sequence and also effectively comparing the kinetics and thermodynamics of sequence-specific and nonspecific DNA−protein interactions with minimal changes in variable.

Before injecting DNA into the subphase, the *P*−*A* isotherm of a fixed amount of only Dps dodecamer was monitored until it reached equilibrium. The stability of the NiA-HisMsDps1 monolayer was also confirmed by checking for an absence of hysteresis in the compression cycles (Figure S4 of Supporting Information). This ensured that the changes we observed after injecting DNA were only due the binding of DNA with His-MsDps1 and rules out any contribution from the free protein molecules. Figure 5a shows the saturation plot for the immobilization of 37 pmoles of dodecameric His-MsDps1 at the NiA monolayer at 25 °C. Figure 5b shows *P*−*A* isotherms for the NiA-His-MsDps1-T7DNA monolayer, when different fractions of DNA were injected relative to the fixed concentration of His-MsDps1 at the same temperature. By assuming that His-MsDps1, on account of its being bound at the monolayer, is responsible for showing surface activity, while T7DNA alone does not

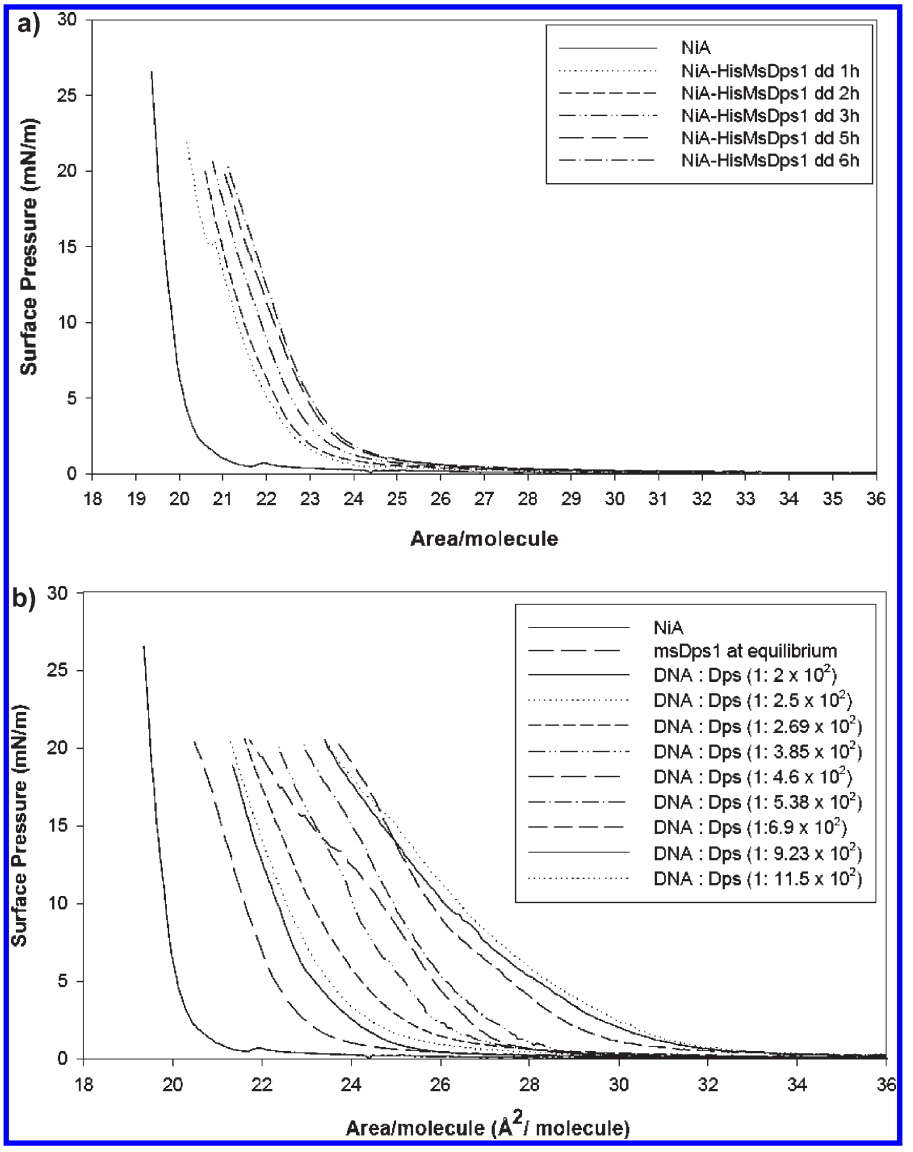

Figure 5. (a) From left to right $P-A$ isotherms of His-MsDps1 dodecamer (37 pmoles) at 25 °C and 20 mM NaCl over a period of 6 h until equilibrium is reached. (b) From left to right $P-A$ isotherms of NiA, NiA-HisMsDps1, and NiA-HisMsDps1 dodecamer with different molar ratio of T7 phage DNA (8.4 nmoles to 42 nmoles) at 10 mM NaCl until saturation is achieved.

have any distinct surface activity, we generated a fractional saturation plot for the binding of DNA with His-MsDps1 until saturation is achieved (Figure 6a). Saturation was reached for a DNA:protein molar ratio of $1{:}10^2-10^3$. The fractional saturation of MsDps1 with DNA was determined using the formula

$$A_t - A_0/A_{max} - A_0 \qquad (2)$$

where A_t is the area per molecule of NiA-Dps-DNA monolayer at any intermediate concentration of DNA. A_0 is the area per molecule of only NiA-Dps. A_{max} is the area per molecule of NiA-Dps-DNA when no more change was observed after the addition of DNA.

The plot was analyzed by fitting to several models of kinetic reactions that reaches saturation,[36] namely,

(a) Rectangular hyperbola, noncooperative binding model: $y = ((ax)/(b+x))$.
(b) Sigmoidal increase to saturation, cooperative binding model: $y = ((ax^n)/(b^n+x^n))$.

The goodness of the fit was judged depending on how close the root mean square (R^2) values were to 1. The binding ratio of Dps to DNA suggests that the protein has multiple binding domains for DNA. If the affinity of identical sites for the same ligand is dependent on each other, we observe a cooperative binding, which gives rise to a sigmoid curve. It is given by the equation

$$\nu = \frac{m[L]^n}{(K_D)^n + [L]^n} \qquad (2.1)$$

where ν is the fractional saturation of the His-MsDps1 by DNA and L is the unbound DNA given by the expression

$$L = L_0 - \nu P_0 \qquad (2.2)$$

L_0 and P_0 are the total DNA and protein concentration, respectively.

dx.doi.org/10.1021/jp209423n |J. Phys. Chem. B 2012, 116, 621–632

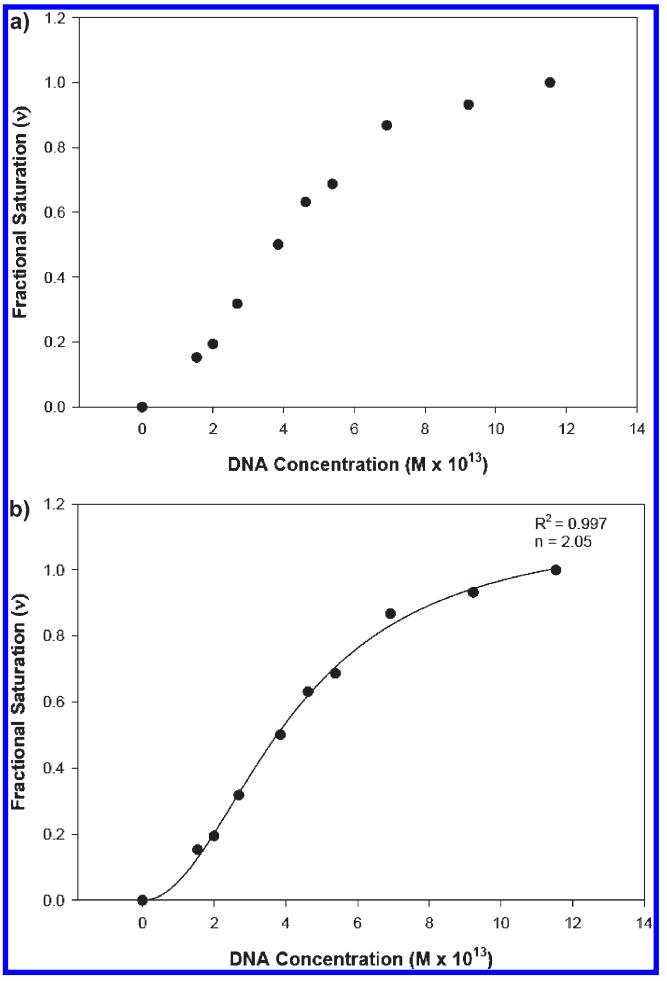

Figure 6. (a) Plot of fractional saturation of His-MsDps1 with DNA as a function of DNA concentration at 25 °C. (b) A Hill Fit for the fractional saturation of His-MsDps1 with DNA at 25 °C. The root mean square (R^2) value was close to 1, and the Hill's coefficient was n = 2.01.

K_D is the apparent dissociation constant and m is the number of binding sites, n is the degree of cooperativity.

However, when the intrinsic affinity of each site, on the substrate, is independent of the other sites i.e., n = 1, eq 2.1 reduces to

$$\nu = \frac{m[L]}{K_D + [L]} \tag{2.3}$$

The above equation follows a rectangular hyperbola model. On rearranging, it gives

$$\frac{\nu}{L} = mK_A - K_A\nu \tag{2.4}$$

which is the equation used to generate a Scatchard plot.

The plot for the fractional saturation of His-MsDps1 with DNA at 25 °C gave a better fit to a sigmoidal model (Figure 6b) than that for a rectangular hyperbola. The initial lag followed by the sudden ramping up in slope is readily explained by increase in the intrinsic binding affinity values for the DNA as the cooperation between the sites increases, resulting in positive cooperativity. The macroscopic dissociation constant (K_D) was determined to be 4.21 ($\pm$0.19) $\times$ 10^{-13} M, and the degree of cooperativity was determined from the Hill coefficient (n) as 2.01. To make sure that the better fit and

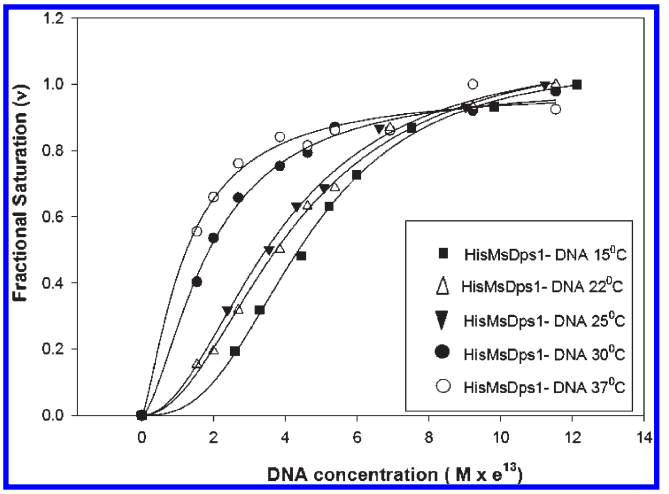

Figure 7. Plots of fractional saturation of His-MsDps1 with T7 DNA at different temperatures.

Table 1. Apparent Equilibrium Dissociation Constants (K_D) for the Interaction of His-MsDps1−DNA at Different Temperatures Obtained by the LB Technique

temperatures [°C]	Hill coefficient [n]	$K_{D,app}$ [M]	ΔG (kcal/mol)
37	1.38($\pm$0.02)	1.23($\pm$0.13) $\times$ 10^{-13}	−17.6
30	1.5($\pm$0.01)	1.89($\pm$0.11) $\times$ 10^{-13}	−17.27
25	2.01($\pm$0.01)	4.21($\pm$0.19) $\times$ 10^{-13}	−17.04
22	2.13($\pm$0.01)	3.85($\pm$0.18) $\times$ 10^{-13}	−17.29
15	2.72($\pm$0.01)	2.72($\pm$0.12) $\times$ 10^{-13}	−17.12

reduced root mean square (R^2) value was not a false positive, obtained because of greater number of variables in Hill fit as compared to a Hyperbolic fit, we also estimated the root mean square values for the fit of RNA polymearase binding to promoter sequence (obtained from our laboratory) using the same two models (Figures S5 and S6 of Supporting Information). It is recorded that RNA polymerase−promoter binding is noncooperative. When the polymerase−promoter binding data was fitted to both the rectangular hyperbolic as well as sigmoidal models, it gave a better root mean square value (0.97) for the rectangular hyperbolic fit. The Hill fit also yielded a Hill's coefficient value close to 1. This indicates beyond doubt that the binding of His-MsDps1 with DNA is co-operative in nature.

To get a detailed idea on the mechanism of binding between the His-MsDps1 dodecamer and DNA, the binding was examined over the temperature range of (15−37)°C. In our previous studies we had already determined that the formation of the NiA monolayer did not show any sensitivity to temperature.[22] In the present case, His-MsDps1 (37 pmoles) at the NiA monolayer was equilibrated at a given temperature before DNA was added. Figure 7 shows the plots for fractional saturation of MsDps1 with DNA over the entire temperature range. Table 1 enlists the macroscopic dissociation constants (K_D) values along with their respective Hill coefficient and calculated free energy (ΔG) values. From the equilibrium constant the Gibbs free energy of reaction (ΔG) was calculated as

$$\Delta G_r = -RT \ln K_A = RT \ln K_D \tag{3}$$

dx.doi.org/10.1021/jp209423n |J. Phys. Chem. B 2012, 116, 621–632

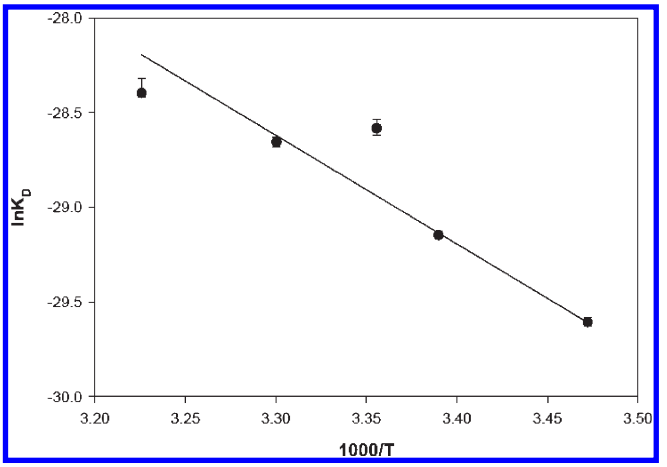

Figure 8. van't Hoffs analysis for the interaction of His-MsDps1 dodecamer with T7 phage DNA at the NiA monolayer.

where R is the gas constant and T is the absolute temperature.

This gave a value of -17.04 kcal mol^{-1} for the free energy of reaction at 25 °C.

Evaluation of Thermodynamic Parameters for His-MsDps1−DNA Interaction. Further, a van't Hoff plot was also constructed over the temperature range of 15−37 °C for the association of His-MsDps1 with T7 DNA (Figure 8) following the equation

$$\ln K_D = \frac{\Delta H}{RT} - \frac{\Delta S}{R} \quad (4)$$

The slope of ln K_D vs $1/T$ provides $\Delta H/R$, from which the enthalpy can be calculated. This equilibrium reaction gave a linear plot over the entire temperature range with an enthalpy value (ΔH) of $-11.6(\pm 0.67)$ kcal mol^{-1}, and value of entropy change (ΔS) was calculated as 19.2 (± 1) cal mol^{-1} K^{-1}. The negative enthalpy value indicates that the MsDps1−DNA interaction is a noncovalent ionic interaction and doesnot involve any DNA melting and breaking of hydrogen bonds ($\Delta H \approx 5$ kcal per mol per base pair). Protein binding to the DNA also involves the release of counterions and water molecules from the DNA backbone that increases the randomness of the system giving a positive entropy value and helps to drive the reaction despite the constraints of a planar environment.

Mechanism of DNA−Protein Interaction for His-MsDps1−DNA Binding. From the above kinetic analysis we conclude that the binding of DNA to His-MsDps1 shows maximum cooperativity (n = 2.72 ± 0.1) at lower temperatures (15 °C), but the degree of cooperativity gradually decreases with increase in temperature (n = 1.38 ± 0.02 at 37 °C). This is surprising as most nonspecific DNA−protein interactions fit a simple single-step binding model.[11] However we should keep in mind that all previous studies were done in the bulk phase, in a homogeneous and dilute solution, where a rapid and reversible equilibrium can be easily achieved. Many reactions behave as pseudo-first-order reactions when studied in a carefully maintained ideal solution where all the species are allowed free exchange, and equilibrium is achieved regardless of the variation in conditions.[37] However, under conditions of nonideality, when kinetic barriers are applied, the same single-step reaction may behave as a multistep process. At the Langmuir monolayer one of the interacting partners is immobilized. The immobilization allows the molecules to retain sufficient mobility such that the intrinsic binding interfaces

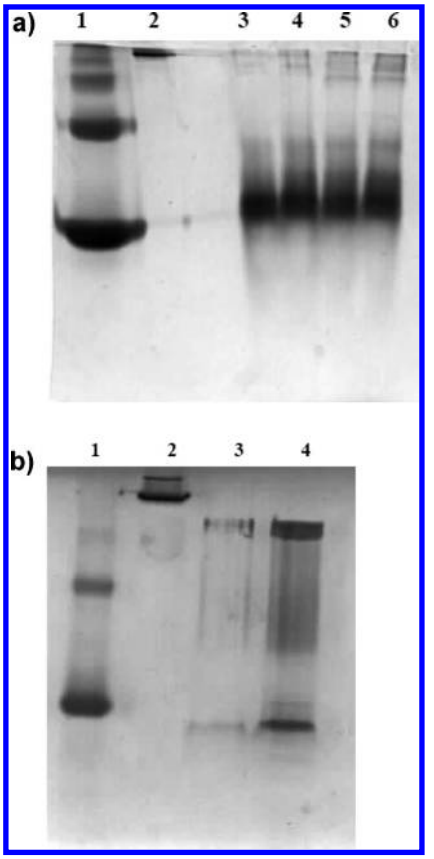

Figure 9. (a) 10% native PAGE of His-MsDps1 trimer, to check the oligomeric status as a function of temperature and pressure. Lane 1, BSA; lane 2, horse spleen ferritin; lane 3, His-MsDps1 trimer at 22 mN/m surface pressure at 25 °C; lane 4, His-MsDps1 trimer with DNA at 22 mN/m surface pressure at 25 °C; lane 5, His-MsDps1 trimer at 22 mN/m surface pressure at 37 °C; lane 6, His-MsDps1 trimer with DNA at 22 mN/m surface pressure at 37 °C. (b) 10% native PAGE of His-MsDps1 dodecamer, to check the oligomeric status as a function of dilution. Lane 1, BSA; lane 2, horse spleen ferritin; lane 3, His-MsDps1 dodecamer in the presence of DNA at 12 mN/m surface pressure at 25 °C; lane 4, His-MsDps1 dodecamer with DNA at 22 mN/m surface pressure at 25 °C.

between two cognate partners is not affected; however, the kinetics of binding may change due to the restriction in the degrees of freedom of the reaction.[38]

To understand the mechanism of DNA binding to His-MsDps1, we should keep in mind that the MsDps1 *in vitro* exists as a structured macromolecular aggregate. His-MsDps1 exists as a trimer with 100% purity at 4 °C in the concentration range of (0.5−5) mg/mL and only converts to its dodecameric form after incubation at 37 °C for 12 h or at very high concentrations of 20 mg/mL, even at lower temperatures (Figure1). Thus the conversion between the two forms is both temperature and dilution driven

$$\text{trimer} \underset{4°C,\ \leq 2\text{mg/mL}}{\overset{37°C,\ 20\text{mg/mL}}{\rightleftharpoons}} \text{dodecamer} \quad (4.1)$$

However, irrespective of the conditions applied, the dodecamer always spontaneously equilibrates with its trimeric form.[39] It has also been observed that the dissociation of the dodecamer into its trimer is further accelerated upon extended incubation at 4 °C.

dx.doi.org/10.1021/jp209423n |*J. Phys. Chem. B* 2012, 116, 621–632

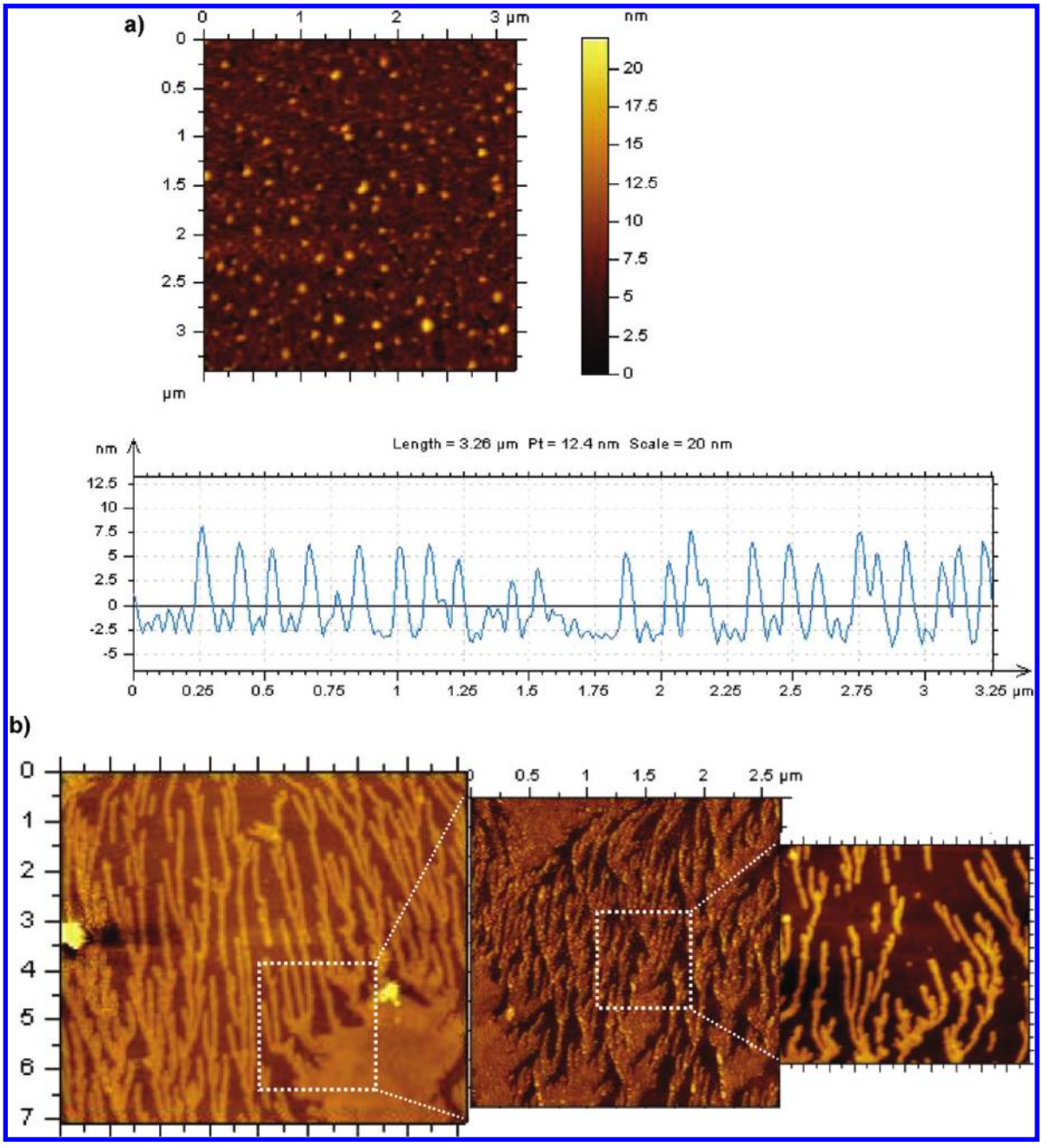

Figure 10. (a) A 3 × 3 μm AFM image of His-MsDPs1 dodecamer on 3 layers of NiA along with a height distribution profile of the image. (b) A 7 × 7 μm AFM image of His-MsDps1 dodecamer with T7 phage DNA on 3 layers of NiA. Sections are zoomed in for better visualization of the two-dimensional network.

When the His-MsDps1 dodecamer is injected into the Langmuir monolayer it undergoes a 100-fold dilution. It is possible that an instantaneous equilibrium occurs between the dodecamer and trimer, wherein a fraction of the dodecamer may dissociate reversibly into its lower oligomeric form with such dilution. When the monolayer is gradually compressed the instantaneous concentration of His-MsDps1 molecules increases and the equilibrium is favored toward the dodecameric form. Again, only the dodecamer has the interface to bind DNA; thus when DNA is injected into the monolayer, it will further shift the equilibrium toward a dodecamer. To check this hypothesis, we transferred the LB monolayer of pure trimer in the absence and presence of DNA at temperatures of 25 and 37 °C, at a constant pressure of 22 mN/m. The His-tagged protein/protein−DNA complex was eluted out of the NiA monolayer using 500 mM imidazole and run on 10% native gel to detect the oligomeric conditions of the protein (Figure 9a). It showed that the pure trimer at 25 °C does not show any equilibrium with its dodecameric form even in a condensed state of the monolayer (22 mN/m). The same trimer in the presence of DNA shows traces of dodecamer formation. This equilibrium is more evident at a higher temperature of 37 °C (lane 5 and 6). However, when the same experiment was done with the dodecamer, in the presence of DNA, we found that the dodecamer has rapidly equilibrated with its lower oligomeric

dx.doi.org/10.1021/jp209423n |*J. Phys. Chem. B* 2012, 116, 621–632

Table 2. Comparison of Kinetic and Thermodynamic Parameters for RNA Polymerase−Promoter Binding and MsDps1−DNA Binding as Obtained from the LB Technique

RNA polymerase−T7A1 promoter binding	MsDps1 dodecamer−T7 DNA binding
sequence-specific in nature, single binding site on polymerase which recognizes DNA consensus sequence	non-sequence-specific in nature, Multiple binding domains on protein with general affinity for DNA backbone
binding ratio of polymerase to DNA, 1:1	binding ratio of MsDps1 to DNA, $1{:}10^2-10^3$
restricted mobility at Langmuir monolayer allowed detection of transient intermediates in the open and closed complex formation $R + P \underset{k_{-1}}{\overset{k_1}{\rightleftharpoons}} RP'_C \underset{k_{-2}}{\overset{k_2}{\rightleftharpoons}} RP_C \underset{k_{-3}}{\overset{k_3}{\rightleftharpoons}} RP'_0 \underset{k_{-4}}{\overset{k_4}{\rightleftharpoons}} RP_0$	reduced degree of freedom showed MsDps1−DNA binding consists of multiple equilibria trimer $\underset{\text{dilution, temp}}{\overset{\text{conc, DNA}}{\rightleftharpoons}}$ dodecamer $\rightleftharpoons$ DNA
apparent dissociation constant (K_D) in the range of 10^{-10} M	apparent dissociation constant (K_D) in the range of 10^{-13} M
for a single strong binding site on the protein, binding was noncooperative, despite kinetic bottlenecks	for multiple binding domains on the protein, binding showed cooperativity when equilibrium was frozen
enthalpy value of $\Delta H = 13.6(\pm 3.6)$ kcal mol^{-1} indicates large conformational change in polymerase and energy required for DNA melting and H-bond breaking ($\Delta H \approx 5$ kcal per mol per base pair)	enthalpy value of $\Delta H = -11.6(\pm 0.67)$ kcalmol^{-1} indicates energy is released from noncovalent ionic interaction with DNA backbone, no conformational change in protein
high entropy value of $\Delta S = 83(\pm 12)$ cal mol^{-1} K^{-1} indicates reaction is entropy driven	entropy value is $\Delta S = 19.2(\pm 1.2)$ cal mol^{-1} K^{-1} only
AFM imaging showed promoter DNA was bound to RNA polymerase at a particular site, and the rest of DNA was linear	AFM studies showed MsDps1−DNA formed a two-dimensional network

form (Figure 9b), irrespective of the degree of compression it is subjected to. This clearly indicates that, for the dodecamer, a rapid and instantaneous equilibration is achieved with its trimer. Thus, when high surface pressure is applied and DNA is also present, the equilibrium is driven toward the dodecamer which then shows DNA binding. Hence, instead of observing a simple single-step DNA−protein binding, we may be observing a multistep eqilibria involving the conversion from trimer toward dodecamer, which then binds DNA.

$$\text{trimer} \underset{\text{dilution, temp}}{\overset{\text{conc, DNA}}{\rightleftharpoons}} \text{dodecamer} \rightleftharpoons \text{DNA} \qquad (4.2)$$

At low temperatures, the degree of dissocation into the trimer will be higher, and the conversion to its dodecameric form becomes the rate limiting step, giving rise to cooperative binding. However when greater thermal energy is provided in terms of increase in temperature, where dodecamer formation is favored, the kinetics moves toward a simple noncooperative binding.

AFM of Dps-DNA LB Monolayer. The binding of His-MsDps1 at the NiA monolayer and its interaction with DNA was further confirmed by visualizing it under AFM. Three layers of NiA were transferred on a hydrophilic glass slide to make it hydrophobic and also to prevent any nonspecific adsorption of proteins. A single layer of the NiA-His-MsDps1/NiA-His-MsDps1−DNA monolayer was then transferred to this preformed glass slide at a constant surface pressure of 22 mN/m. Prior to imaging the proteins the 3 layers of NiA were characterized by AFM and the root mean square roughness was found to be within 0.7 nm (Figure S7 of Supporting Information), which is much smaller than the dimensions of the protein molecules being investigated (9 nm). The imaging of several microscopically separated areas showed the presence of globular structures with uniform dimensions in the range of 7.5−10.5 nm (Figure 10a). This value corresponds closely with the dimensions of dodecameric Dps as obtained from the crystal structure ($9 \times 9 \times 9$ nm).[29] However when AFM images were taken for the NiA-Dps-DNA monolayer, no array formation was observed. Instead, we observed an extensive two-dimensional network with a uniform height profile of 12.5 nm (Figure 10b). The presence of this network also provides evidence that the Dps−DNA interaction at the monolayer doesnot involve interaction between isolated dodecameric units and the DNA but is a concerted process to give rise to a highly organized two-dimensional network.

Comparison of Kinetics and Thermodynamics of Sequence-Specific and Nonspecific DNA Protein Interaction. The study of DNA−protein interaction at an interface brings to light some interesting observations. The constrains imposed by immobilization of the molecules at the LB monolayer, along with other kinetic barriers, showed us that the MsDps1−DNA binding is not completely reversible. In this regard, a comparison with sequence-specific RNA polymerase−promoter recognition studies[22] may be necessary in order to highlight the subtle differences in the DNA recognition of both nonspecific and cognate partners. For both cases of DNA−protein binding, the generation of a kinetic bottleneck allowed us to trap intermediates in an otherwise reversible equilibrium. For RNA polymerase recognizing a single consensus sequence the binding is always noncooperative with an apparent dissociation constant (K_D) of 10^{-10} M, while the nonspecific multidomain interaction of MsDps1 with DNA resulting in a layered array had a cooperative binding with K_D in the range of 10^{-13} M. The cognate partner binding involves conformational changes on the protein resulting in a positive enthalpy value [$\Delta H = 13.6(\pm 3.6)$ kcalmol^{-1}], while a nonspecific binding only involves ionic interactions [$\Delta H = -11.6(\pm 0.67)$ kcalmol^{-1}]. Spectroscopically, the RNA-polymerase−promoter binding showed the DNA is attached at a

single point and each polymerase-promoter complex exists as a separate entity (Figure S8 of Supporting INformation), while in the case of MsDps1−DNA binding we observed the formation of a organized two-dimensional network (Figure 10b). The major similarities and differences between the two different modes of DNA−protein interaction are further detailed in Table 2.

CONCLUSION

The immobilization of His-MsDps1 at the LB monolayer and the characterization of its properties give us some important observations. The different oligomeric forms of the protein can be layered on a LB film, and the ferroxidation activity of the protein as well as the ability of the dodecameric form to physically bind DNA is not altered. The LB technique provides a unique, physiologically compatible, two-dimensional technique to follow DNA−protein interaction at an interface. Our bulk phase studies may provide valuable information regarding the mechanism of a biological reaction, but the kinetics obtained from such a quasi-physiologically adapted system often results in incomplete information. The immobilization of one of the interacting components in order to generate macromolecular crowding provides a more practical approach in our attempts to closely resemble the in vivo environment. The ionic strength used at the LB monolayer is less compared to that used in bulk phase studies of similar interactions. However, one should keep in mind that the requirement of ionic strength in restricted environment is different, and salt concentration used was sufficient to prevent nonspecific adsorptions and intramolecular/intermolecular aggregation and precipitation at the subphase. No previous study has been done on His-MsDp1s-DNA binding affinities even in solution. However this nonsequence-specific DNA−protein interaction is similar in nature to the formation of nucleosomes and their condensing effect on DNA. There are reports of similar cooperativity being observed in the case of DNA−histone interactions when the equilibrium was frozen in the presence of high salt, while the kinetics followed noncooperative binding when a dilution fit was followed.[40] Further, for the same set of experiments the data is reproducible. The amount of sample required to generate a sensitive response is also very low compared to other spectroscopic techniques. We believe that LB technique has far-reaching biological as well as technological implications in studying protein−DNA interactions in vitro.

ASSOCIATED CONTENT

Supporting Information. Additional experimental data for a detailed understanding of this work is included. Protein purification of His-MsDps1. *P*−*A* isotherms of NiA, showing sensitivity to pH, salt, and temperature. AFM images of NiA. A schematic of the Y-type hydrophilic transfer of LB monolayer on glass slides. This material is available free of charge via the Internet at http://pubs.acs.org.

AUTHOR INFORMATION

Corresponding Author

*E-mail: dipankar@mbu.iisc.ernet.in. Phone: +91-80-22932836. Fax: +91-80-23600535.

Present Address

‡S.N. Bose National Centre for Basic Sciences, Sector III, Block JD, Salt Lake, Kolkata 700 098, India

ACKNOWLEDGMENT

D.C. thanks Department of Science and Technology, Government of India, for sponsored projects. A.G. and S.M.W. thank CSIR for SRF fellowship. We would like to acknowledge Subho Ghosh for the AFM Spectroscopy and Mr. I. S. Jarali, Department of Solid State and Structural Chemistry Unit, IISc for FTIR Spectroscopy.

REFERENCES

(1) Von Hippel, P. H.; McGhee, J. D. *Annu. Rev. Biochem.* **1972**, *41*, 231–300.
(2) Alberts, B.; Johnson, A. Lewis, J. Raff, M.; Roberts, K.; Walter, P.; *Mol. Biol. Cell*; 4th ed.; New York, Garland Science; 2002.
(3) Hawley, D. K.; McClure, W. R. *Nucleic Acids Res.* **1983**, *11*, 237–2255.
(4) Mangiarotti, L.; Cellai, S.; Ross, W.; Bustamante, C.; Rivetti, C. *J. Mol. Biol.* **2009**, *385*, 748–760.
(5) von Hippel, P. *Science* **2004**, *305*, 350–352.
(6) Kalodimos, C. G.; Biris, N.; Bonvin, A. M. J. J.; Levandoski, M. M.; Guennuegues, M.; Boelens, R.; Kaptein, R. *Science* **2004**, *305*, 386–389.
(7) Paull, T. T.; Haykinson, M. J.; Johnson, R. C. *Genes Dev.* **1993**, *7*, 1521–1534.
(8) Roe, J. H.; Burgess, R. R.; Record, M. T., Jr. *J. Mol. Biol.* **1985**, *184*, 441–453.
(9) Rosenberg, S.; Kadesch, T. R.; Chamberlin, M. J. *J. Mol. Biol.* **1982**, *155*, 31–51.
(10) Johnson, R. S.; Chester, R. E. *J. Mol. Biol.* **1998**, *283*, 353–370.
(11) von Hippel, P. *Science* **1994**, *263*, 769–770.
(12) Frenkiel-Krispin, D.; Ben-Avraham, I.; Englander, J.; Shimoni, E.; Wolf, S. G.; Minsky, M. *Mol. Microbiol.* **2004**, *51*, 395–405.
(13) MacBeath, G.; Schreiber, S. L. *Science* **2000**, *289*, 1760–1763.
(14) Hu, Y.; Das, A.; Hecht, M. H.; Scoles, G. N. *Langmuir* **2005**, *21*, 9103–9109.
(15) Volker, J.; Breslaur, K. J. *Annu. ReV. Biophys. Biomol. Struct.* **2005**, *34*, 21–42.
(16) Tsoi, P. Y.; Yang, M. *Biosens. Bioelectron.* **2004**, *19*, 1209–1218.
(17) Bhaumik, A.; Ramakanth, M.; Brar, L. K.; Raychaudhuri, A. K.; Rondelez, F.; Chatterji, D. *Langmuir* **2004**, *20*, 5891–5896.
(18) Gaines, G. L. *Insoluble Monolayers at Liquid-Gas Interfaces*; Wiley- Interscience: New York, 1966.
(19) Hinterdorfer, P.; Dufrêne, Y. F. *Nature Methods* **2006**, *3*, 347–355.
(20) Brar, L. K.; Rajdev, P.; Raychaudhuri, A. K.; Chatterji, D. *Langmuir* **2005**, *21*, 10671–10675.
(21) Ganguly, A.; Chatterji, D. *Langmuir* **2011**, *21*, 10671–10675.
(22) Ganguly, A.; Rajdev, P.; Chatterji, D. *J. Phys. Chem. B* **2009**, *113*, 15399–15408.
(23) Almiron, M.; Link, A. J.; Furlong, D.; Kolter, R. *Genes Dev.* **1992**, *6*, 2646–2654.
(24) Krispin, D. F.; Zaidman, S. L.; Shimoni, E.; Wolf, S. G.; Wachtel, E. J.; Arad, T.; Finkel, S. E.; Kolter, R.; Minsky, A. *EMBO* **2001**, *20*, 1184–1191.
(25) Krispin, D. F.; Avraham, I. B.; Englander, J.; Shimoni, E.; Wolf, S. G.; Minsky, A. *Mol. Microbiol.* **2004**, *51*, 395–405.
(26) Gupta, S.; Pandit, S. B.; Srinivasan, N.; Chatterji, D. *Protien Eng* **2002**, *15*, 6503–6511.
(27) Gupta, S.; Chatterji, D. *J. Biol. Chem.* **2003**, *278*, 5235–5241.
(28) Roszak, D. B.; Colwell, R. R. *Microbiol. Rev.* **1987**, *51*, 365–379.
(29) Roy, S.; Gupta, S.; Das, S.; Sekar, K.; Chatterji, D.; Vijayan, M. *J. Mol. Biol.* **2004**, *339*, 1103–1113.
(30) Nierman, W. C.; Chamberlin, M. J. *J. Biol. Chem.* **1979**, *254*, 7921–7926.
(31) Laemmli, U. K. *Nature* **1970**, *227*, 680–685.
(32) Rajdev, P.; Chatterji, D. *Langmuir* **2007**, *23*, 2037–2041.

(33) Roy, S.; Ramachandran, S.; Gupta, S.; Sekar, K.; Chatterji, D.; Vijayan, M. J. *Mol. Biol.* **2007**, *370*, 752–767.
(34) Leirmot, S.; Harrison, C.; Cayley, D. S.; Burgess, R. R.; Record, M. T., Jr. *Biochemistry* **1987**, *26*, 2095–2101.
(35) Castle, A. M.; Macnab, R. M.; Shulman, R. G. *J. Biol. Chem.* **1986**, *261*, 3288–3294.
(36) Cantor, C. R.; Schimmel, P. R. *Biophysical Chemistry: Part III: The Behaviour of Biological Macromolecules*; W.H. Freeman and Company, 1980.
(37) Shoemaker, G. K.; Soya, N.; Palcic, M. M.; Klassen, J. S. *Glycobiology* **2008**, *18*, 587–592.
(38) Wu, Y.; Vendome, J.; Shapiro, L.; Ben-Shaul, A.; Honig, B. *Nature* **2011**, *475*, 510–513.
(39) Ceci, P.; Ilari, A.; Falvo, E.; Giangiacomo, L.; Chiancone, E. *J. Biol. Chem.* **2005**, *280*, 34776–34785.
(40) Thåström, A.; Gottesfeld, J. M.; Luger, K.; Widom, J. *Biochemistry* **2004**, *43*, 736–741.